

Evaluation of accelerated, forced-convection cooling methods for sinter-hardening of low-alloy steels

Zbigniew Zurecki and Lisa Mercando,

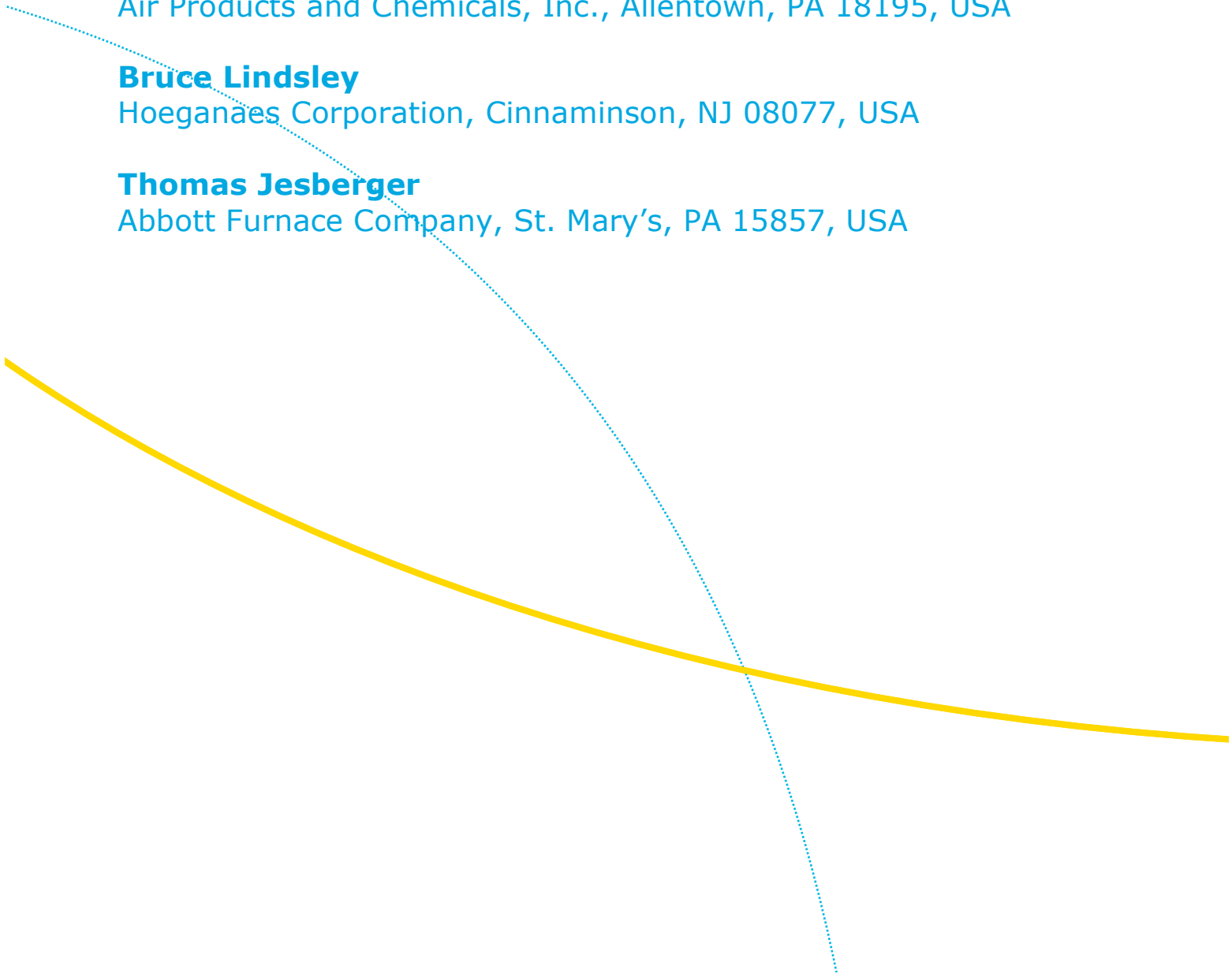
Air Products and Chemicals, Inc., Allentown, PA 18195, USA

Bruce Lindsley

Hoeganaes Corporation, Cinnaminson, NJ 08077, USA

Thomas Jesberger

Abbott Furnace Company, St. Mary's, PA 15857, USA



Abstract

The success of sinter-hardening depends on cooling rate (CR) achieved in the forced-convection zone, and if that rate is limited, steel powders used must contain elevated levels of expensive alloying additions for enhancing hardenability. Apart from lowering material cost, accelerated CR may result in reduced dimensional distortion (due to reduced hardenability of lean alloys used) and a shortened furnace footprint, if a more effective cooling system complements the conventional, blower/water heat exchanger unit. Focused on maximizing CR, lab and production-scale test studies were undertaken to explore the quenching and transformation hardening capacity of cryogenic as well as high-velocity gas jets impinging on the surface of sintered, low-alloy gears kept at austenitic temperature. Oil and liquid nitrogen bath quenching were used as a benchmark. This paper outlines the lab and field test results evaluated in terms of CRs measured, apparent hardness, distortion, and microstructure.

Introduction

Sinter-hardening is a well-established commercial technology combining sintering and forced-convection gas quenching of martensitic steels in one continuously processing furnace. It is valued for its cleanliness and process integration that, eventually, translate into reduced operating and capital costs. However, the quenching rates of the atmospheric-pressure, forced convection cooling systems used in typical sintering furnaces are limited if compared to the conventional oil bath quenching, and this creates an issue when considering sinter-hardening of lower-cost, lean-alloyed powder metallurgy (PM) steels. Production and processing of lean-alloy steel parts, with shipments directed largely to the automotive industries, is presently a hot industrial topic, and several industrial research groups and companies explore a partial or complete substitution of expensive molybdenum and nickel with a combination of chromium, manganese, and silicon and with carbon adjustments¹⁻⁸. Such substitutions necessitate improved powder processing techniques because the reactivity of Mn and/or Cr exceeds that of Mo and/or Ni, and the compressibility of Mn and/or Cr alloyed powders is typically lower. Nitrogen-hydrogen rather than endothermic sintering atmospheres provide a remedy to the first problem. The lean-alloyed steels are also less hardenable, which lessens the problem of thermal distortion during quenching, but may result in an unacceptable drop in the strength and wear resistance of the product. Consequently, new and more effective convection cooling systems are required for maximizing martensitic transformation during quenching by increasing the cooling rate. Reported gas quenching studies⁹⁻¹¹ offered a starting framework. Two heat transfer mechanisms are involved in the quenching of just sintered parts on their entry into the convective cooling system: radiative cooling that scales with part temperature to the fourth power, i.e., becomes less significant at lower temperatures, and the Newton's law-based convective cooling:

$$dQ/dt = h A \{T(t) - T_{\text{coolant}}\}$$

where: Q is the thermal energy transferring from the hot part to the surrounding coolant, h is the heat transfer coefficient produced at the interface between the part surface and the cooling medium, A is the contact surface area between the part and the cooling medium, T is a time-dependent temperature of the part (or at least its surface), and T_{coolant} is the temperature of the cooling medium in contact with the part surface. Modern convection cooling systems use water-jacketed, black internal walls to address the radiative cooling requirement and an external water heat exchanger that, combined with a blower, recirculate cooled gas back to the quenched steel parts in a predesigned pattern, Figure 1. Following Newton's law, the most critical portion of metal quenching depends on the temperature of the gas leaving the water heat exchanger and the gas velocity that affects the heat transfer coefficient. Two ways available for accelerating convective cooling are the use of a much colder cooling medium and enhancing the heat transfer coefficient which always scales with the impingement velocity of cooling medium. The use of a cryogenic cooling medium, such as liquid nitrogen (LIN) and its cryogenic vapor, is one option, but its circulation inside the unit would also chill the cooling water, resulting in poor refrigeration efficiencies. Additionally, industrially supplied LIN comes in high-pressure cylinders or can be easily pressurized without the use of a pumping system, which means that discharging it from nozzles directly at quenched parts may result in a heat transfer coefficient higher than that characterizing the conventional blower-powered convective cooling units. Injecting LIN directly above the furnace belt that carries PM parts and pre-atomizing it in nozzles into a spray may increase anticipated cooling efficiency by involving an in situ evaporation, with the enthalpy of LIN boiling, ΔH , thus, contributing to the heat-and-mass balance. To exemplify the effect, if LIN evaporates and its vapor is subsequently

heated to 550°C (1020°F) inside the convective cooling unit, LIN enthalpy of boiling will contribute nearly 20% to the overall refrigeration effect. Although the outlined concept of direct impingement cooling is attractive from the heat transfer standpoint, a number of questions must be answered before applying it in sinter-hardening operations. Thus, it is not clear if the martensitic transformation of lean-alloyed PM parts will be uniform in their entire cross section, and if the one-sided impingement proposed would result in thermal distortion. To be cost-effective, an inventive cryo-spraying system should also utilize as few nozzles as possible, i.e., the number of impingement spots per each PM part will have to be limited, which leads to a reduced contact area, A_j , between the jet or spray and the part surface, and may further contribute to distortion and/or insufficient transformation as discussed elsewhere¹²⁻¹⁴. Finally, given the high temperature of the parts quenched, the Leidenfrost¹⁵ and liquid jet burn-back effects may result in an unexpectedly reduced heat transfer coefficient, h , within an already reduced contact area between the jet and the part.

With these questions in mind, the following 2-step development program was set forth for exploring the feasibility of martensitic quenching of lean-alloy PM steels using direct impingement cooling methods:

1. Laboratory-scale examination of impingement quenching applied to already sintered PM parts combined with comparative evaluation of structures and properties produced by competing cooling methods.
2. Verification of direct impingement cooling methods in a fully loaded, industrial-scale sinter-hardening furnace.

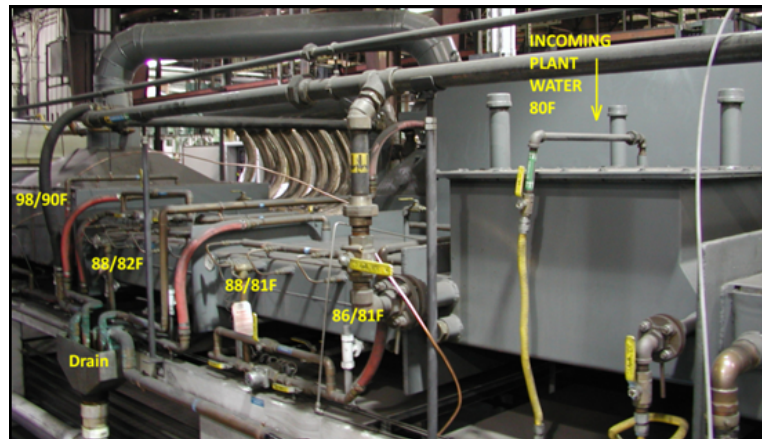


Figure 1. Water-jacketed Varicool convection cooling system installed on a large-sized sinter-hardening furnace (courtesy of Abbott Furnace Co.).

I. Laboratory-scale exploration

1.1 Experimental procedures

A batch of flat sprocket gears, 280 grams and 3.9 inch dia. (0.1 m) each, was pressed to the density of 7.0 g/cm³ using a manganese-molybdenum alloyed powder (ANCORBOND FLM-4000) supplied by Hoeganaes Corp. Thus, 0.75 wt % graphite and 0.5 wt % Acrawax lubricant were added to the base composition comprising nominally 1.25 wt % Mn, 0.5 wt % Mo, and 0.1 wt % O. Green parts were sinter-hardened conventionally, under a N₂-10 vol % H₂ atmosphere, in a production furnace using a belt speed of 6 in/min (2.5 mm/s) according to the thermal profile presented in Figure 2.

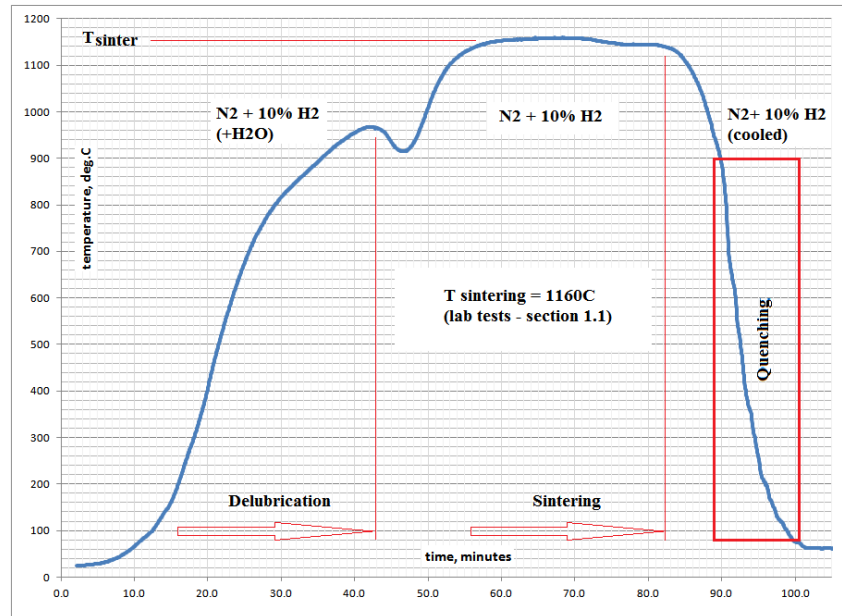


Figure 2. Typical temperature profile applied in sinter-hardening operations.

Composition and microstructure of sinter-hardened gears, shown in Figure 3, have been found to be sufficient for carrying out the quenching portion of this program. There was a 10% variation of metallic components between the gears analyzed, perhaps resulting from an accidental contamination of the present powder batch with another, and 5% variation of carbon between the four gears analyzed. This and a somewhat limited degree of sintering and diffusion of elements were corrected later, during our industrial demonstrations that involved, also, an increase in sintering temperature.

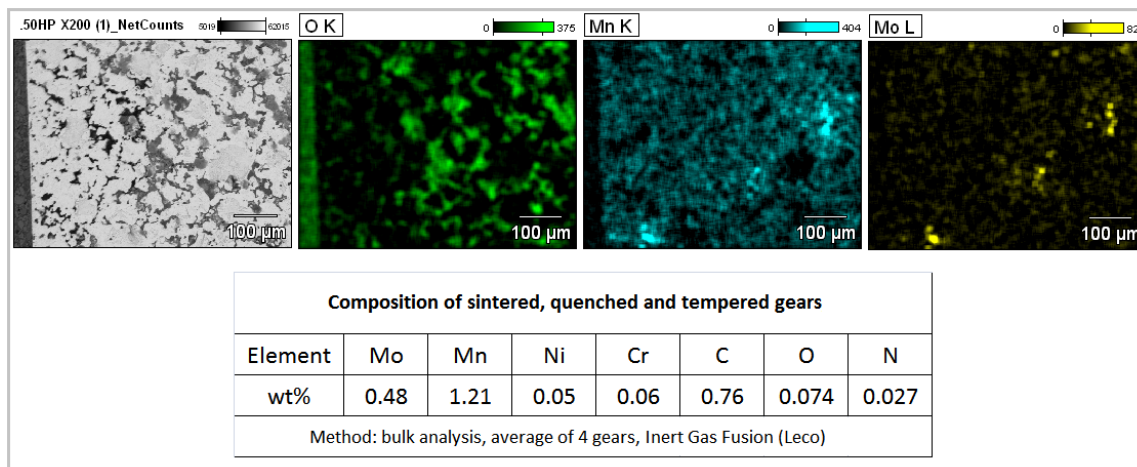


Figure 3. Elemental distribution (SEM/EDS) and averaged bulk composition of sinter-hardened gears.

The sinter-hardened gears were subsequently austenitized in a box furnace at 860°C (1580°F) under the atmosphere of N₂-0.1 vol % CH₄ for 0.5 hrs, then, quenched for martensitic transformation using the following four methods listed in Table 1. Such mild austenitizing conditions were selected to preserve the original sinter-hardened and tempered microstructure along with its characteristic hardening response. In the last step, one set of gears was examined in the resultant “as-quenched” condition, and the other set was additionally tempered at 200°C under the atmosphere of pure N₂ and cooled with furnace before the final examination.

Listed in Table 1, the martensitic quenching methods explored included an oil bath as a popular heat-treating benchmark; LIN bath (liquid nitrogen at 1 atm. pressure) for transforming retained austenite below the M_f - temperature if any was formed; quenching under multiple streams of room-temperature gas to simulate typical operations of the conventional convection cooling units comprising a water heat exchanger, such as Abbott's *Varicool*; and quenching using a single jet of expanding liquid N_2 spray in order to evaluate the viability of a cryo-jet quenching method. The supply of cooling medium to the surface of the quenched gear is, theoretically, unlimited in the first two methods, but the vapor envelope formed during liquid boiling significantly reduces effective heat fluxes and cooling rates. The effect is especially prolonged and significant in the case of the LIN bath, which continuously boils until the quenched gear reaches -195°C . The supply of cooling medium to the metal surface in the last two methods was limited by flow control valves to 1 kg/min in order to provide a fair comparison and ensure viable economics in the large-scale, commercial applications.

Table 1: Gear Quenching Methods Explored

Method	Description	Cooling medium temperature
1	Oil Bath – quenching by rapid immersion in an oil tank	$+50^\circ\text{C}$
2	LIN Bath – quenching by rapid immersion in a liquid N_2 tank	-195°C
3	Multi-jet – quenching under 3 streams of low-pressure N_2 gas	$+20^\circ\text{C}$
4	LIN-jet – quenching under a single jet of liquid N_2 spray	$+195^\circ\text{C}$ at the nozzle exit

All gears tested had embedded thermocouples (TC) installed. Figure 4 shows the schematic of jet quenching procedure. Gears were removed from the box furnace at austenitic temperature and placed on a belt moving at 6 in/min (2.5 mm/s) in ambient air to be driven under stationary quenching nozzles located 3.5 inches (0.09 m) above the belt surface. In the case of method 3, three jets of room-temperature nitrogen gas were impinged on the gear surface in a symmetric pattern shown below. However, in the case of method 4, only one jet was used, and its traversing path over the gear was selected to be asymmetric. This test strategy considered the fact that method 3 simulates the operation of a blower-driven convective cooling unit, where the quenching gas can be recycled multiple times, so that large numbers of nozzles and volumes of gas may be impinged on a metal surface economically. In contrast, the cryogenic temperature of N_2 can't be economically restored during recycling; therefore, the LIN consumption during jetting has to be limited. An additional argument for using only one jet during direct LIN impingement was the desire to retain the 2-phase (liquid/gas) jet composition. If the jetted mass-flow rate of 1 kg/min were to be divided into many miniature spray jets, sprayed droplets would be expected to evaporate on the way from the nozzles to the metal surface inside the real sinter-hardening furnaces.

In all tests, the top side of the gears was the top side during the pressing green parts. This top side was face-up during the sinter-hardening operation and, later, during the jet quenching. Tracing the original top/bottom side orientation of the gears throughout the test program was important for assessing possible processing errors such as a density gradient in the green parts and/or decarburizing in the sintering atmosphere. Further chemical and structural gear analyses have shown that decarburization was completely absent; hence, the differences between the top and bottom sides could be related only to the pressing and/or jet quenching operations.

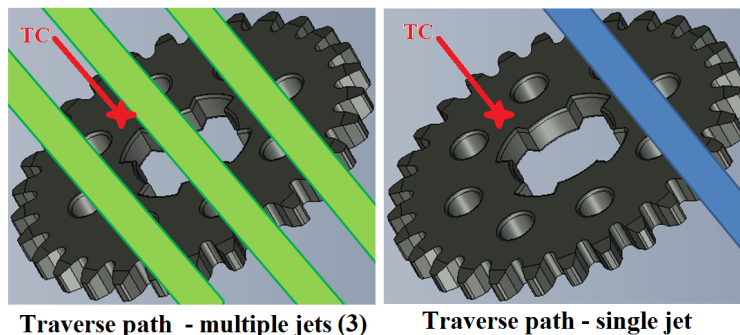


Figure 4. Single- and multiple-jet quenching patterns applied to austenitized gears.

Apparent hardness (Rockwell C-scale) of each gear was measured in 4 locations (0, 90, 180 and 270 degrees apart) on both sides and on four corresponding teeth. Hardness averages and standard deviation were computed for each cooling method. Metallographic samples of the teeth adjacent to the embedded thermocouples were cut to show the top and the bottom side of the gear. Flatness and dimensional integrity of the quenched and tempered gears were examined using a Starrett optical comparator and a Mitutoyo granite surface plate indicator.

1.2. Lab test results

Figure 5 represents the raw cooling data during quenching. As expected, the oil bath quench appears to be the most effective, which is welcome news for all lean PM alloys characterized by limited hardenability. In contrast, the LIN bath cooling is slow, confirming the anticipated effect of a vapor envelope and bubbling¹⁶ around the quenched gear, although the quench ends at cryogenic temperatures, below the scale of Figure 5. The slopes of the cooling curves are fairly steep for both jet quenching methods 3 and 4, but the quenching terminates abruptly, soon after the belt driven gears move away from the nozzles. Further quenching would take place though, if these nozzles operated inside the conventional, convective cooling unit. A control box is drawn on Figure 5 and Figure 6 for the 550°C–250°C temperature range which has been debated in literature as one of the possibly important ranges during the continuous cooling for minimizing ferritic/pearlitic and bainitic transformations and producing purely martensitic structures¹⁷⁻²⁰. As seen in Figures 5 and 6, the average cooling rate of the LIN-jet is of about the same order as the cooling rate of the oil quench within this specific temperature range. The supreme cooling rates of oil²¹ are realized mostly at the higher temperatures, where the austenitic phase of the quenched PM alloy is still stable. Consequently, benefits of fast quenching, starting at the temperatures as high as 950°C or 850°C could be sought mainly in a potentially improved retention of alloying additions in the metal matrix, reduced precipitation of alloy carbides and, subsequently, an enhanced hardening response of the metal, which is so important in lean-alloyed systems. Figure 7 shows that the LIN-jet and the oil bath quench cooling rates are also about the same within the broader 600°C–200°C range, while the cooling methods 2 and 3 offer significantly lower CR values. However, the impact of cooling rates on as-quenched and tempered metal hardness (HRC) is somewhat muted, Figure 8. For an arbitrary benchmark level of 36 HRC, only the LIN-bath quenched gear falls below, and only in its tempered condition. Clearly, fast cooling rates are the key in sinter-hardening of the 1.25Mn–0.5Mo–0.75Gr alloy tested, while sub-zero treatments for the conversion of retained austenite are not critical.

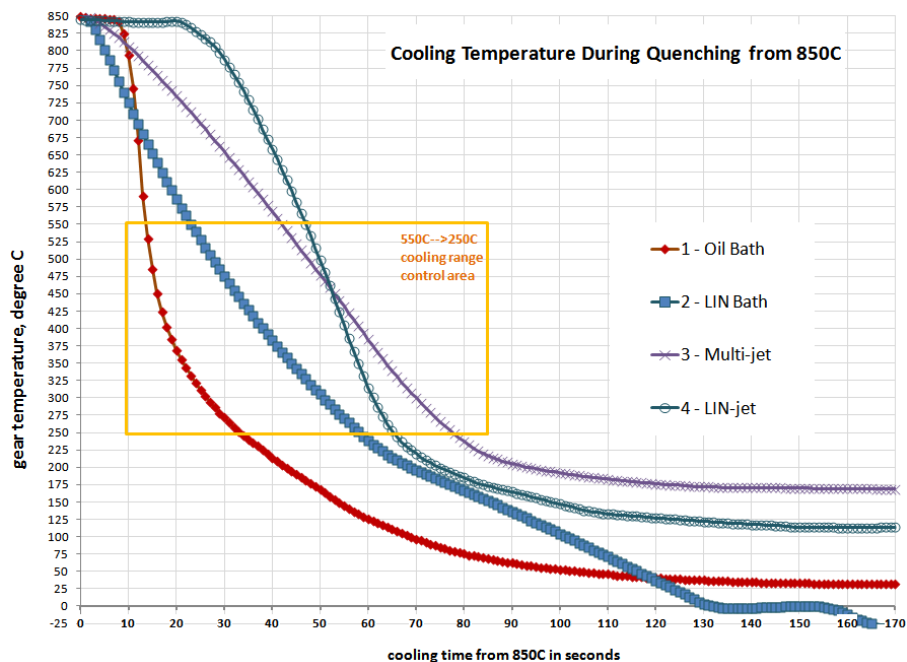


Figure 5. Profiles of gear temperature as a function of cooling time from 850°C (1560°F) in seconds.

The higher apparent hardness of the bottom side of the most gears tested was investigated further. The standard deviation between HRC values calculated separately for the bottom and the top gear sides were about the same: 2–3 HRC points. This and a fairly uniform extent of martensitic transformation on both sides of the gears, as observed on etched metallographic samples, indicated porosity problems. Examination of the gear cross sections in as-polished condition confirmed an uneven porosity distribution between the top and the bottom sides. Additionally, a 3D optical microprofiling was carried out on the flat, external surface areas of the sinter-hardened gears, away from the teeth area, which confirmed the density difference, Figure 9. Not surprising in view of the references discussing Mn-rich PM alloys, these results indicate the importance of optimizing the lubrication and pressing procedures.

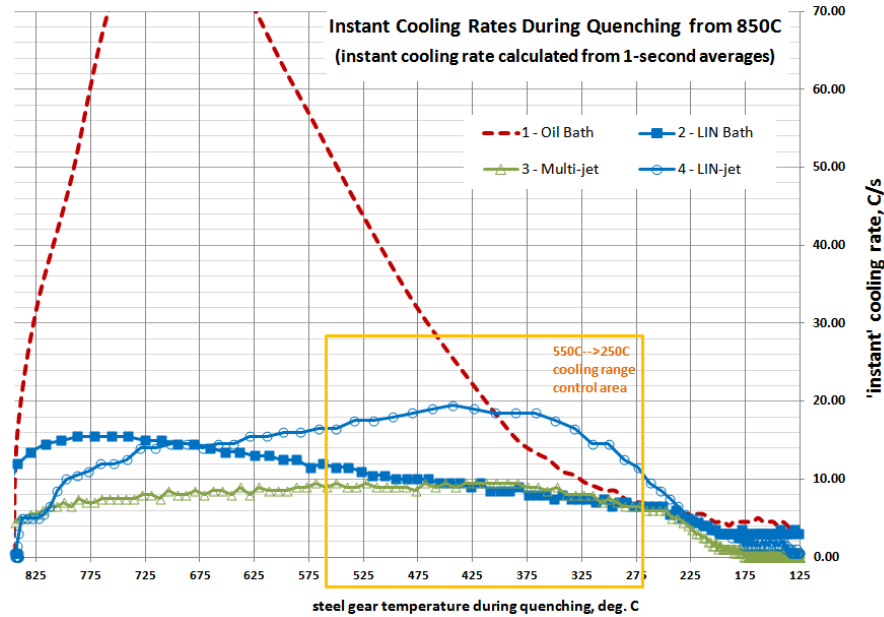


Figure 6. Cooling rates (K/s) as a function of actual gear temperature.

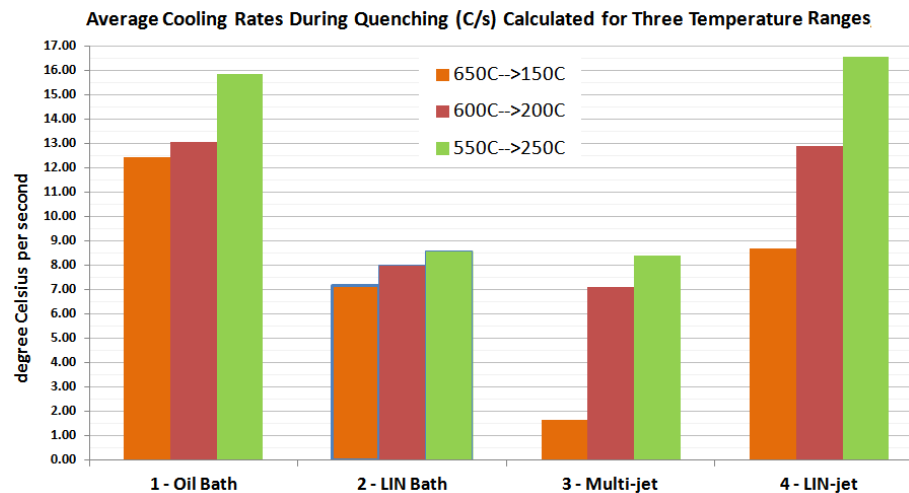


Figure 7. Average gear cooling rates for three arbitrarily selected temperature ranges.

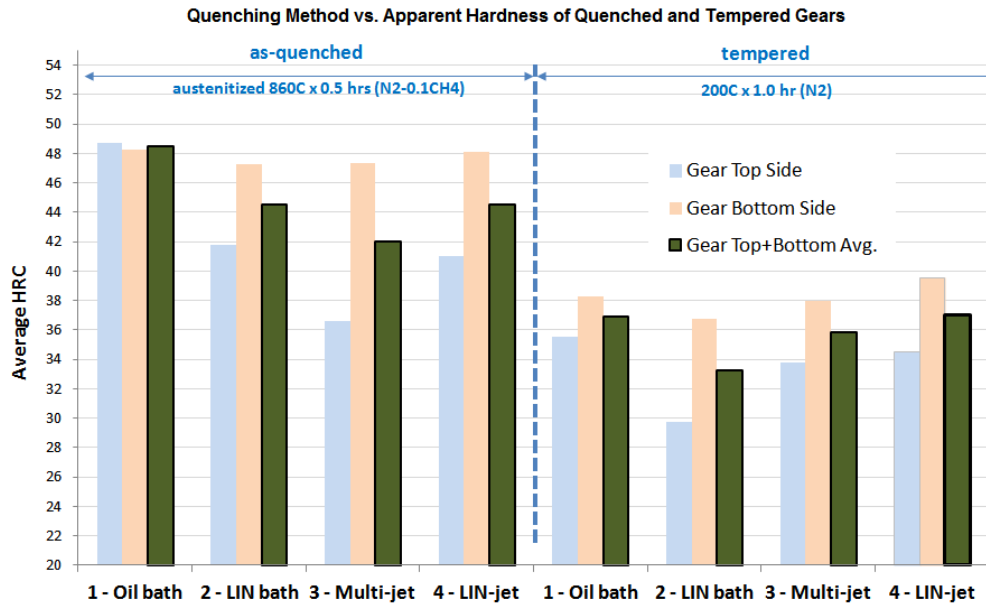


Figure 8. Average values of apparent hardness (Rockwell C-scale) of as-quenched and tempered gears.

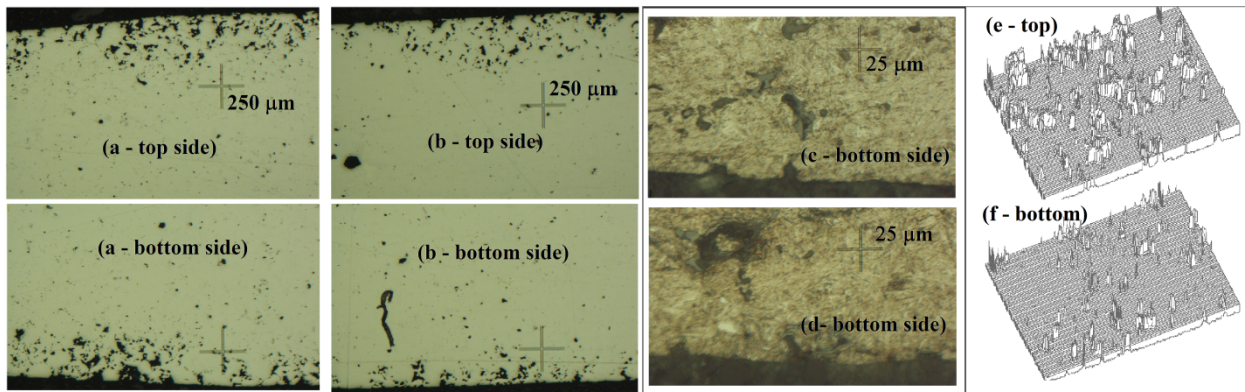


Figure 9. Microstructural evaluation of the quenched gears: (a-d) cross section of the gear tooth after sintering, experimental quenching, and tempering, where *top/bottom side* indicates the top/bottom side in the mold during green part pressing; (a and d) gear quenched using the LIN jet, method 4, (b and c) gear quenched in the oil, method 1. (a-b) As-polished, 50 x orig. magnif. and (c-d) etched in nital, 500 x orig. magnif. (e and f) Optical microprofiles (3D) of the top and the bottom surfaces showing the distribution of open porosity on the external gear surface.

Dimensional stability of the quenched and tempered gears is best with method 3, and worst for the oil and the LIN bath methods. Method 4 falls into the middle. Although all measured dimensional changes are technologically acceptable, a trend can be observed suggesting that severe thermal shock and vapor envelope characterizing bath quenching methods result in larger deformations than jet-cooling methods, even if just one cryogenic jet is asymmetrically impinged on the gear surface. The present finding is further supported by the industrial experience indicating that all forms of gas convective cooling, high-pressure and atmospheric pressure alike, reduce thermal distortions normally observed during liquid bath quenching.

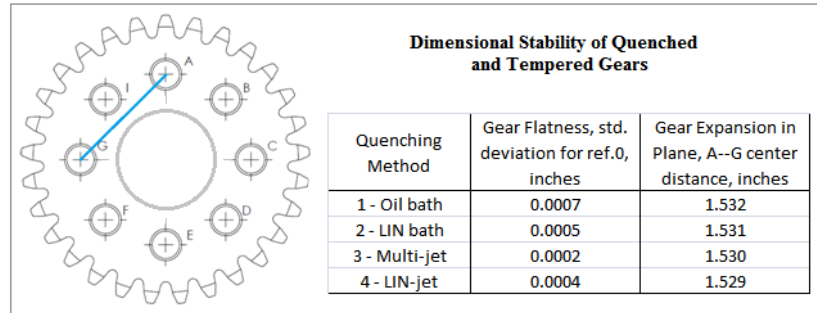


Figure 10. Flatness and longitudinal changes in quenched and tempered gears.

There are several conclusions drawn from this part of the present study. A complete martensitic transformation of individual gears made of the lean, 1.25%Mn–0.5%Mo–0.75%Gr alloy is feasible using room-temperature as well as cryogenic gas jets and spray cooling methods adoptable inside sinter-hardening furnaces. The cooling rates and the transformation performance of the LIN-jet quenching method matches that of the oil bath quenching within the temperature range important for the austenite-to-martensite transformation. Dimensional stability of the gears quenched is affected by immersion (bath) cooling, and much less by impingement jetting. It’s an apparent result of a significantly higher thermal conductivity of the sintered bulk than the surface heat transfer coefficient under the jet, and indicates that a thin boundary film forming on the metal surface during the LIN impingement is predominantly gaseous and uniform. These findings suggest that a liquefied or gaseous jet-quenching method can be successfully applied to individual steel parts processed in automated manufacturing cells. However, it is still not clear how effective the method can be in quenching of a full load in industrial sinter-hardening furnaces. The following section of the present study focuses on this aspect of quenching.

2. Industrial-scale demonstration

2.1. Test methodology

Industrial-scale cryogenic jet cooling tests were carried out using a large sinter-hardening furnace built by Abbott Furnace Co. and equipped with a *Varicool*, blower-driven convective cooling unit. Manifolds with LIN spray-jetting nozzles were installed inside the *Varicool* on the entry side, not far from the end of the sintering zone. Two proprietary designs of LIN sprayers with nozzle diameters optimized in a similar manner, as in reference 22, were tested individually and side by side: L- and S-types. A Ni- and Cu-free alloy 1.25%Mn–0.5%Mo–0.75%Gr (Powder A), tested in the previous part of this study, and a blend substituting Cu for Mn, 0.5% Mo–1.0Cu–0.85%Gr (Powder B) were used for pressing and sinter-hardening the gears configured as previously shown. In earlier industrial sinter-hardening trials, the Mn-containing alloy was found to transform to a martensitic-bainitic structure, whereas the Cu-containing alloy was fully bainitic and did not contain martensite. The gears were loaded on a 36 inch wide (0.91 m) belt of the furnace to the production capacity of about 500 lbs/hr (227 kg/hr). With the stainless steel mesh belt and the ceramic support plates for the sintered gears moving at 6 in/min (2.5 mm/s), the total mass of hot material entering the convective cooling unit was estimated to reach 1000 lbs/hr (454 kg/hr). Preliminary evaluations of the heat-and-mass balances inside the cooling unit equipped with LIN jetting system, performed using Fluent CFD, Figure 11, have shown that sufficiently rapid quenching could be obtained when the LIN spray is directed toward the gears and the mesh belt, and carried out concurrently with the normal operation of the *Varicool* unit recirculating N₂–10 vol% H₂ atmosphere across the water-cooled heat exchanger. The sintering temperatures were increased to 1170°C (+/–5°C), higher than for the material tested in the lab. Improvements in uniformity and hardenability of the Mn-containing lean alloy steels, resulting from high sintering temperatures, were reported elsewhere²³⁻²⁸.

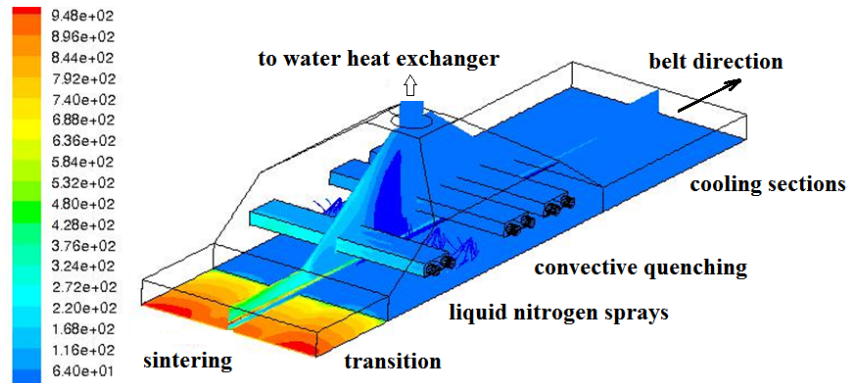


Figure 11. Temperature fields inside the convection cooling unit (*Varicool* of Abbott Furnace Co.) equipped with a LIN-jetting sprayer at the entry end, a Computational Fluid Dynamics (CFD) prediction for one set of quenching conditions.

Each sprayer type was tested using a baseline LIN flow rate and, also, both sprayers were run simultaneously, each at half of the baseline flow. The latter resulted in a reduced intensity of the jet impingement and a doubled contact time between the jets and the surface of gears. Another condition tested involved the baseline flow rate reduced by 25%. Several tests were run using the above conditions. Initially, the apparent hardness of the top and the bottom surfaces of the gears quenched was reported separately, as in the previous part of this study. Later, after observing that all resultant hardness values were around the 40 HRC point and, in a few cases in the mid-forties, it was decided to simply report one average value for the gears run under specific sets of conditions; the decision was based on the industrial product norm for this type of gear that required the as-quenched hardness to reach only the 36–38 HRC threshold level. Figure 12 illustrates the LIN jet impingement in the baseline condition produced by both sprayers: the furnace was empty; therefore, no gears were oxidized during taking these pictures. (In the real operation, LIN jets are turned off as soon as the furnace belt is unloaded.) As planned, the jets expanding inside the furnace were reaching the belt surface without excessive evaporation. The top sides of the gears loaded later were face-up and quenched by the impingement the same way as in the lab tests. The temperature measurement technique used in the industrial tests was different though. The temperature acquired inside the convective cooling unit was the “atmosphere temperature” just above the belt, and not the actual “gear temperature”, because the thermocouple tip was not embedded in the gear but, rather, covered by a hollow metallic dome (shoe). Consequently, there’s no direct match between the cooling rates measured during the lab and the industrial demonstration tests.

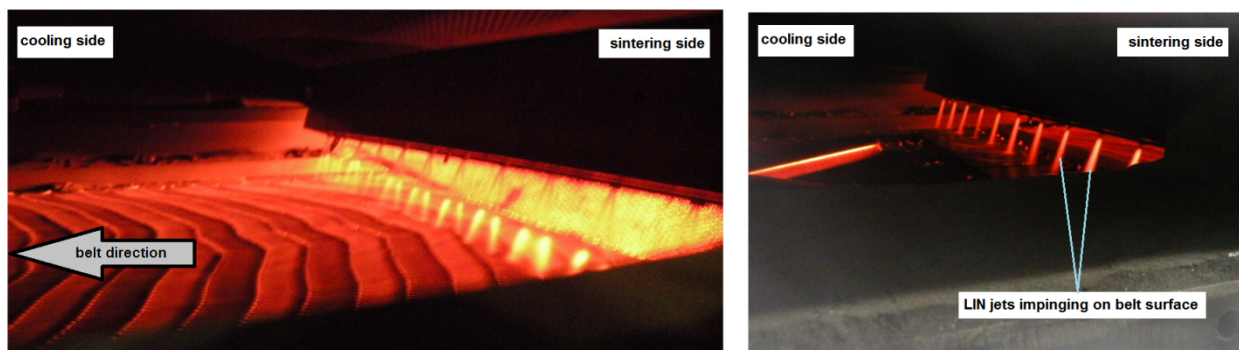


Figure 12. In-furnace operation of the direct LIN-jet impingement sprayers, view inside the convection cooling unit, the L- (left) and S-type (right) sprayers are positioned above the 36”-wide (0.91 m) belt.

2.2. Industrial test results

Due to the difference in the temperature measurement technique, the cooling rates recorded during the industrial tests and reported below for the 565°C–204°C range (1050°F–400°F) were lower than those found in the lab testing. Nevertheless, the as-quenched hardness was comparably high, suggesting a complete or a nearly complete martensitic transformation and the actual cooling rates of the metal under the LIN jets approached the value of approximately 7–8 K/s (13–14 °F/s). Table II shows, that after optimizing powder blending and pressing procedures, the ratio between the top/bottom surface hardness became more unified, with the tops typically harder. A somewhat slower cooling of the ceramic plate supports on which the gears were placed during the sinter-hardening might have contributed to this effect. In spite of these somewhat different apparent hardness levels between the top and the bottom sides, subsequent dimensional measurements proved that all quenched gears were well within the specification.

Table 2: Belt Cooling Rate and Apparent Gear Hardness (HRC) for Different Spraying Arrangements

	Test a		Test b		Test c		Test e		Test e	
Top/Bottom Side HRC Distribution for 2 Powder Grades	S-sprayer, Base Flow rate		S-sprayer, 75% of Base Flow rate		L-sprayer, Base Flow rate		Repeated Test c		S-and L-sprayers Combined to Base Flow rate	
Belt Cooling Rate (K/s)	4.0		3.4		4.0		4.0		2.0	
Gear Side:	Top	Bottom	Top	Bottom	Top	Bottom	Top	Bottom	Top	Bottom
Powder A	43	39	44	39	44	42	46	41	46	41
Powder B	43	44	44	44	40	37	44	39	40	39

Comparing tests a to b shows that although the cooling rate calculated from the gas temperatures is lower for the lower LIN flow rate, the hardness of the impinge-quenched gears is about the same. Hence, the LIN mass flow rate could be further optimized in the future. The as-quenched HRC data scatter observed during testing can be attributed to a combination of factors, such as the metal temperature gradient during cooling, uniformity of powder blending and porosity distribution, as well as variability in the cooling rates across the width of the belt. The sprayer configurations, S, L, and S+L are comparably effective within this range of experimental error. Halving the dynamic impingement pressure while doubling the gear residence time under the LIN jets appears, then, to be another acceptable option for both alloys tested. What is worth stressing is a starkly different transformation response for the convective cooling with and without LIN impingement: earlier industrial sinter-hardening tests, carried out in the same furnace and using the same loaded belt procedure, have shown that the average cooling rate in the same 565°C–204°C range (1050°F–400°F) was only 1.5 K/s, and the average gear hardness measured for Powder A was only 27 HRC, less than the 36–38 HRC threshold required when run without LIN impingement.

Further testing illustrated the key difference between the cooling profiles for the baseline LIN mass-flow rate and the profiles for the 25% reduced mass-flow rate, Figure 13. Thus, the temperature slopes in the critical martensitic transformation range were fairly similar, but the exit temperatures of the gears moving away from the *Varicool* into the slow cooling zones, near the furnace end, were higher in the case of the reduced flow rate. Nevertheless, the as-quenched hardness of these gears was about the same for both quenching conditions and alloys tested. This result shows that assuring fast cooling rates in the range below 150°C aren't necessary, and further LIN mass-flow rate optimization strategies are possible in order to produce additional process savings. Alternatively, the depressed exit temperature of the gears cooled with the baseline flow rate can be used to significantly shorten the length of the slow cooling zones, i.e. reduce the footprint of the entire furnace. Furnace length creates serious issues in quite a few PM plants running sinter-hardening and even the most basic, sintering operations.

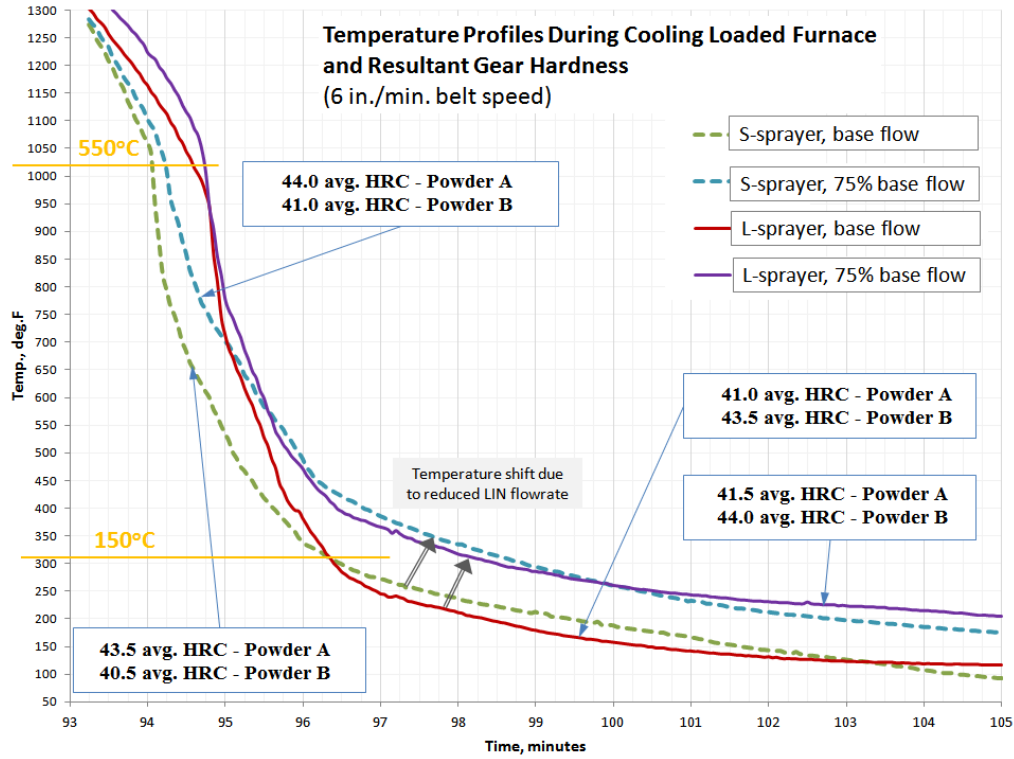


Figure 13. Profiles of the temperature of gas atmosphere just above mesh belt during sinter-hardening as a function of cooling time.

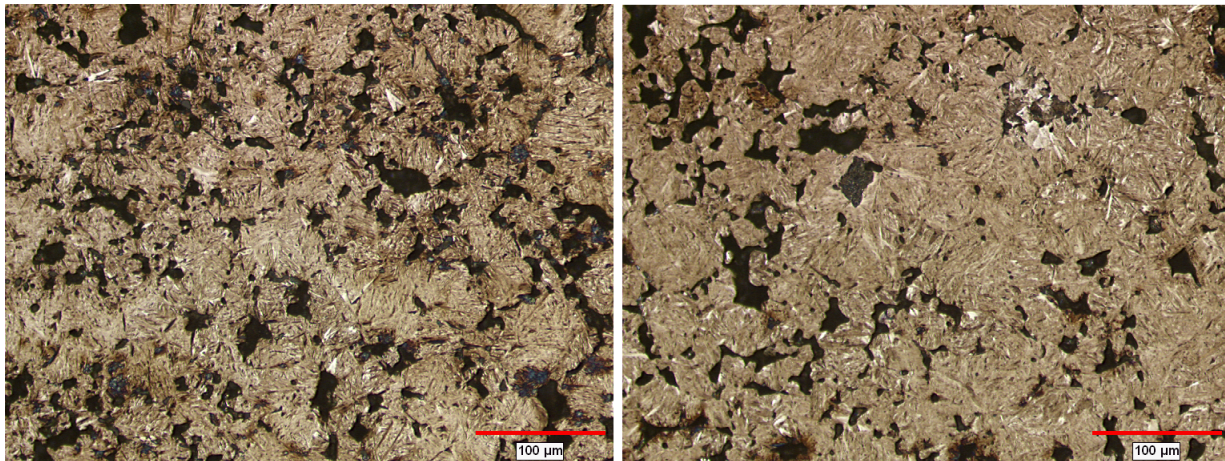


Figure 14. Optical microscopy of sinter-hardened gears made of Powder A (left) and Powder B (right), Test c, Table 2. Etched using 2% nital/4% picral.

Figure 14 presents typical microstructures of the gears quenched using the test c condition (Table 2). The gears have a good degree of sinter, and their microstructures are predominately martensitic. To summarize, recorded cooling rates, as-quenched hardness, and steel microstructures show that the direct cryogenic impingement, applied inside a concurrently operating, conventional blower-driven convection cooling unit, can produce good quality lean-alloy parts, even with a production-scale loading of a sinter-hardening furnace.

Concluding remarks

A direct cryogenic jet-quenching method was evaluated in both laboratory and industrial production environments as a means for accelerated cooling and martensitic transformation of less-hardenable, lean-alloyed PM steels. The extent of the transformation was found to be excellent by the industrial norms and comparable to that of oil bath quenching, but without the thermal distortions associated with the latter. PM parts, e.g., gears, configured as flat disks appear to be most suitable for the present jet quenching. Industrial implementation of this new sinter-hardening method requires retrofitting or replacing existing convection cooling units and will be followed. Shorter belt furnace cooling zones can also be used with this method, and smaller, conventional sintering furnaces can be adopted for sinter-hardening operations.

Acknowledgments

The authors would like to thank John Green, Dave Nelson, and Xiaoyi He of Air Products for their dedicated support in the designing, fabricating, and modeling of the prototype LIN sprayers and the execution of the test program.

References

1. M. Campos et al., "Sintering behavior improvement of a low Cr-Mo prealloyed powder steel through Mn additions and other liquid phase promoters", *J. of Materials Proc. Technology*, 143-144 (2003) 464-469.
2. Z. Zhang and R. Sandstrom, "Fe-Mn-Si master alloy steel by powder metallurgy processing", *J. of Alloys and Compounds*, 363 (2004) 194-202.
3. Klekovkin et al., "Heat Treatment of Cr-Mo Powder Metallurgy Steels for high Performance Applications", *Proc. of the 24th ASM HT Soc. Conf.*, Sept. 17-19, 2007.
4. P. Sokolowski et al., "Lean can mean sinter-hard and cost-effective", 40 *Metal Powder Report*, July/August 2008, Elsevier metal-powder.net.
5. B. Lindsley, "Sinter-Hardening Response of Leaner Alloy Systems", *Advances in Powder Metallurgy & Particulate Materials* (2009), MPIF
6. E. Hryha et al., "Surface composition of the steel powders pre-alloyed with manganese", *Applied Surface Science* 256 (2010) 3946-3961.
7. M. Selecka and A. Salak, "Industrial Sintering of Hybrid Low-Carbon 3Cr-0.5Mo-xMn Steels", Vol. 46, Issue 4 (2010), *International J. of Powder Metallurgy*.
8. U. Engstrom et al., "Cost Effective Material for Heat Treated Gear Applications", *Proc. of the EURO PM2011*, Barcelona, Oct. 10, 2011.
9. J. Ferrari et al., "An evaluation of gas quenching of steel rings by multiple-jet impingement", *J. of Materials Proc. Technology*, 136 (2003) 190-201.
10. N. Lior, "The cooling process in gas quenching", *J. of Materials Proc. Technology*, 155-156 (2004) 1881-1888.
11. A. Malas et al., "A New Approach to Sintering Furnace Atmosphere Control and Sinter Hardening by Gas Impingement Cooling", *Advances in Powder Metallurgy and Partic.*, Vol. 2, PP 05-41-54, 2008.
12. S. Schuttenberg et al., "Controlling of Distortion by means of Quenching in adapted Jet Fields", *Mat.-wiss. u. Werkstofftech.* (2006), 37, No. 1, 92, Wiley-VCH Verlag GmbH.
13. M. Brzoza et al., "Minimizing Stress and Distortion for Shafts and Disks by Controlled Quenching in a Field of Nozzles", *Mat.-wiss. u. Werkstofftech.* (2006), 37, No. 1, 97, Wiley-VCH Verlag GmbH
14. A.S. Sabau and A. Wu, "Evaluation of a heat flux sensor for spray cooling for the die casting process", *J. of Materials Proc. & Technology* 182 (2007) 312-318.
15. Ali Hashmi et al., "Leidenfrost levitation: beyond droplets", *Scientific Reports*, Macmillan Publishers Limited. | 2 : 797 12 Nov. 2012 pp. 1-4.
16. M. Maniruzzaman and R. Sisson, "Bubble Dynamics During Quenching of Steel", 21st ASM HT Soc. Conf. Proc., 5-8 Nov. 2001, Indianapolis, IN, ASM Intl.

17. F.J. Semel, "Cooling Rate Effects on the Metallurgical Response of a Recently Developed Sinter Hardening Grade", PM2TEC 2002, International Conf. on Powder Metallurgy & Particulate Materials, June 16-21, 2002, Orlando, FL, USA.
18. S. Hatami et al., "Critical aspects of sinter-hardening of prealloyed Cr-Mo steel", J. of Materials Proc. Technology 210 (2010) 1180-1189.
19. R. Dziurka and J. Pacyna, "The influence of carbon content on the kinetics of phase transformations of undercooled austenite of the Cr-Mn-Mo model alloys", Archives of Material Sci. & Engr., Vol. 47, Issue 2, Feb. 2011, pp. 77-84.
20. C. Larsson et al., "High Performance Sinter Hardening Materials for Synchronizing Hubs", EURO PM2011, Barcelona, Oct. 10, 2011.
21. ASM Specialty Handbook, Carbon and Alloy Steels (ed. by J.R. Davis), ASM Intl., p. 150, 1996.
22. D. H. Lee et al., "The Effect of Nozzle Diameter on Impinging Jet Heat Transfer and Fluid Flow", Trans. of the AIME, 554/Vol. 126, Aug. 2004.
23. A. Salak et al., "Manganese in Ferrous Powder Metallurgy", Powder Metallurgy Progress, Vol. 1 (2001). No 1, pp. 41-58.
24. H. Danninger et al., "Degassing and deoxidation Processes During Sintering of Unalloyed and Alloyed PM Steels", Powder Metallurgy Progress, Vol.2 (2002), No 3, pp. 125-140.
25. E. Hryha et al., "Critical Aspects of Alloying of Sintered Steels with Manganese", Metallurgical and Materials Transactions A, Vol. 41A, Nov. 2010, pp. 2880-2897.
26. M. Sulowski et al., "Microstructure and Properties of Cr-Mn Alloyed Sintered Steels:", Powder Metallurgy Progress, Vol. 12 (2012), No 2, pp.71-83.
27. E. Hryha et al., "On-line control of processing atmospheres for proper sintering of oxidation-sensitive PM steels", J. of Materials Processing Technology 212 (2012) 977-987.
28. D. Chasoglou et al., "Effect of process parameters on surface oxides on chromium-alloyed steel powder during sintering", Materials Chemistry and Physics 138 (2013) 405-415.

For more information,
please contact us at:

**North America, Corporate
Headquarters**

Air Products and Chemicals, Inc.
7201 Hamilton Boulevard
Allentown, PA 18195-1501
T 800-654-4567
T 610-706-4730
F 800-272-4449
F 610-706-6890
Email gigmrktg@airproducts.com

Air Products Asia, Inc.

1001, 10/F, Sunning Plaza
10 Hysan Avenue, Causeway Bay
Hong Kong
T +852-2527-1922
F +852-2527-1827
infoasia@airproducts.com

Europe

Air Products PLC
Hersham Place Technology Park
Molesey Road
Walton-on-Thames
Surrey K12 4RZ
UK
T +44-0-1270 614 314
Email apbulkuk@airproducts.com



tell me more
airproducts.com/metals